XLIV Jornadas de Automática 2023

https://jautomatica.es

# A model-independent constrained predictive control for the Furuta Pendulum

Martínez, B. V.*, Sanchis, J., García-Nieto, S.

*Departamento de Ingeniería de Sistemas y Automática, Universitat Politècnica de Valencia, Camino de Vera, nº14, 46022, Valencia, España.*

**To cite this article:** Martínez, B. V., Sanchis, J., García-Nieto, S. 2023. A model-independent constrained predictive control for the Furuta Pendulum.
XLIV Jornadas de Automática, 323-328. https://doi.org/10.17979/spudc.9788497498609.323

**Resumen**

Este trabajo presenta el control de seguimiento de un péndulo Furuta basado en el diseño de dos lazos paralelos con restricciones, rechazo activo de perturbaciones y predicción de salidas. Para cada subsistema, se asume que la planta gobernada tiene una dinámica de primer orden más integrador (FOPI). Así, se calcula una ley de control predictivo aplicando una estrategia de horizonte deslizante en dicha planta (FOPI). La diferencia entre la dinámica real y el modelo de predicción asumido se compensa mediante el mecanismo de rechazo de perturbaciones heredado del control activo de rechazo de perturbaciones (ADRC) e incorporado en los lazos. Para el diseño del control no se realiza ninguna identificación de modelos ni linealización matemática. Además, la estrategia permite incorporar las restricciones reales del sistema. Este trabajo valida con resultados prometedores la arquitectura denominada *Modified Active Disturbance Rejection Predictive Control* (MADRPC) mediante la estabilización de un sistema mecánico sub-actuado considerando las variables restringidas y en ausencia de un modelo nominal, en contraste con el enfoque estándar en el Control Predictivo de Modelos (MPC) en espacio de estados.

*Palabras clave:* Rechazo activo de perturbaciones, Control predictivo, Sistemas con restricciones, Control multivariable.

**Control predictivo con restricciones e independiente de modelo para el péndulo de Furuta.**

**Abstract**

This paper presents the tracking control of a Furuta pendulum based on the design of two parallel-constrained loops with active disturbance rejection and outputs predictions. For each subsystem, it is assumed that the governed plant resembles first-order plus integrator (FOPI) dynamics. So, a predictive control law is computed by applying a receding horizon strategy in such FOPI plant. The mismatch between the actual dynamics and the assumed prediction model is compensated through the disturbance rejection mechanism inherited from the Active Disturbance Rejection Control (ADRC) incorporated in the loops. No modelling identification or mathematical linearisation is performed for the control design. Moreover, the strategy allows the incorporation of the actual system constraints. This work validates with promising results the architecture named Modified Active Disturbance Rejection Predictive Control (MADRPC) by stabilising a sub-actuated mechanical system considering the constrained variables and in the absence of a nominal model, in contrast to the standard approach in the state-space Model Predictive Control (MPC).

*Keywords:* Active Disturbance Rejection Control, Predictive Control, Constrained systems, Multivariable control.

## 1. Introduction

When proposing new control architectures, either by introducing novel approaches, additional features to existing techniques or integrating attractive strategies in the form of composite control, the validation phase is mandatory, and for this purpose, varied benchmarks resembling challenging dynamics are usually selected.

Comprising the above group are the inverted pendulums whose behaviour is considered descriptive of many applications with unstable, non-linear, and non-minimum phase features.

*Corresponding author: blamarca@doctor.upv.es

Indeed, these processes are of the sub-actuated type, so configurations with two control loops are commonly preferred (Hamza et al., 2019).

On the one hand, there is the cascaded loop, where internal control is designed to maintain the pendulum in its unstable position based on the measured deviation from the vertical. This controller is driven by a virtual reference angle for the pendulum provided by the external control loop designed to control a cart or an arm to which the pendulum is attached. On the other hand, a parallel configuration can be implemented by designing a controller that computes a driving signal for stabilising the pendulum, which is combined with the signal determined for a controller related to the base.

Either of the above strategies is commonly implemented with control methodologies independent of the process model, like the Proportional-Integral-Derivative (PID) control or the Active Disturbance Rejection Control (ADRC) (Han, 2009). For example, (Ramírez-Neria et al., 2014) uses a tangent linearisation around an equilibrium point to design high-order extended linear observers for the cascaded control of a Furuta Pendulum. This approach is also the base of the proposal in (Ramirez-Juarez et al., 2021) for a double pendulum gantry crane.

From another perspective, the works of (Liu et al., 2019) and (Chen et al., 2022) address an improvement in the non-linear function of the non-linear ADRC formulation to better compensate for the discrepancies between the dynamics of a cart inverted pendulum and the integrator chain commonly assumed as the modified plant in the ADRC methods. The benefits of switching between the non-linear and linear ADRC are also presented for the aforementioned sub-actuated system in (Xian et al., 2020), and more recently, (Onen, 2023) studied the combination of the Extended State Observer (ESO) from ADRC with PID control and Sliding Mode Control (SMC) for this type of benchmark.

Another attractive option, however, is the complete control of the sub-actuated system through its linearised model, as is the case of the Model Predictive Control (MPC) proposals from (Seman et al., 2013) and (Madrid et al., 2019). Other works such as (Prado et al., 2020), (Homburger et al., 2022), and (Diwan and Deshpande, 2022) have extended the model-based control to the non-linear analysis by the study of the Non-linear MPC for the Furuta pendulum in an attempt to reduce the effect of the non-modelled features.

The ADRC and the MPC may be considered opposed control strategies. The former keeps the required plant information to the minimum, and the latter bases its development on correctly identifying a nominal model, which brings to discussion the possibility of integrating both approaches. This is the idea behind the Modified Active Disturbance Rejection Predictive Control (MADRPC) (Martínez, 2023). A control architecture where a predictive control law is designed assuming that the governed plant is a fixed state-space realisation of a first-order plus integrator system. Moreover, the design incorporates constraints for the system requirements and conditions for feasibility and stability. The prediction model is then constructed by estimating the states of the assumed plant based on the input-output information and an approximation of the nominal critical gain and the time constant of that modified system.

This work presents the implementation of the MADRPC in a Furuta Pendulum selected as case study and which constitutes a laboratory set-up for experimentation available at the Department of Systems Engineering and Automation from the Polytechnic University of Valencia. Two main research goals are addressed here.

- The MADRPC strategy is validated through its use to control a highly non-linear mechanical system.
- The MADRPC approach is adapted to a process resembling a sub-actuated plant with more outputs than inputs.

Simulation results in a multi-body 3D environment show that a control loop in parallel configuration can be designed for the Furuta pendulum, assuming that each controlled variable is governed by an independent MADRPC loop, highlighting that

- No linearised or detailed model information is required for the implementation. Instead, the open-loop response of the process can be analysed to extract the initial values of the needed tuning parameters.
- The design process is considered straightforward and intuitive and provides satisfactory results. However, if the performance requirements play a crucial role in the design, a more dedicated tuning procedure may be beneficial.

The structure of this work is as follows. Section 2 introduces the non-linear dynamics of the Furuta Pendulum and the mechanical analysis performed to approximate its behaviour with simulation tools. Section 3 recalls the formulation of the constrained loop with active disturbance rejection and outputs prediction to control the rotary inverted pendulum. Consequently, the design and adaptation of the MADRPC approach for the Single-Input Multiple-Output (SIMO) system under study are presented in Section 4 with the simulation results obtained. Finally, Section 5 draws the main conclusions and future research directions.

**Symbols and nomenclature**

| | |
|---|---|
| $c$, $p$ | control and prediction horizon |
| $\lambda$, $\gamma$ | weighting factors for prediction error and input rate |
| $\epsilon_1$, $\epsilon_2$ | weighting factors for slack variables |
| $\underline{w}$, $\overline{w}$ | lower and upper bound for variable $w$ |
| $b_0$, $T$ | nominal value of critical gain and time constant |
| $\omega_o$ | observer bandwidth |
| $t_s$ | sampling time |
| $x_{i\|k}$ | future value at instant $k+i$ based on conditions at $k$ |

## 2. Furuta Pendulum: a non-linear sub-actuated system

The Furuta pendulum (FP) is a rotary inverted pendulum constituting a multi-variable system. An arm can rotate in a horizontal plane where its rotation angle $\theta$ is measured viewed from the superior plane. At the end of the arm, a bar hanging freely emulates the oscillatory movement of a pendulum describing an angle $\alpha$ in a vertical plane from the front view.

Tabla 1: Parameters of the Furuta pendulum

| | Description | Units |
|---|---|---|
| $m_p$ | Mass of pendulum | kg |
| $L_a$ | Length of arm | m |
| $L_p$ | Length of pendulum | m |
| $l_p$ | Position of the pendulum centre of mass | m |
| $J_a$ | Moment of inertia of arm | kg/m$^2$ |
| $J_p$ | Moment of inertia of pendulum | kg/m$^2$ |
| $C_p$ | Damping coefficient for pendulum | N m s/rad |
| $k_\tau$ | Electromotive torque constant of motor | N m/A |
| $R_m$ | Electrical resistance of motor | Ω |

Both angles are controllable. However, the system is considered sub-actuated because these outputs respond to a single input representing the torque applied by a motor axis joined to the arm, possibly through a gearbox. The voltage $v$ in the motor terminals is the actuation signal which determines the turn direction and the achievable arm velocity.

The dynamics analysis of the Furuta pendulum reveals that it is a highly coupled non-linear system, and consequently, it represents a benchmark for the validation of control strategies.

### 2.1. *Non-linear dynamics*

The Furuta pendulum modelling is commonly obtained through the Euler-Lagrange formulation based on the energies analysis or the Newton-Euler iteration methodology based on forces and moments (Cazzolato and Prime, 2011). Any of the two approaches leads to the ordinary differential equations describing the angular acceleration $\ddot{\theta}$ of arm and angular acceleration $\ddot{\alpha}$ of pendulum as functions of the angles, velocities, voltage input and mechanical parameters.

According to the above, the Furuta pendulum dynamics are governed by (1)-(2). The complete description of the parameters is listed in Table 1.

$$\left(J_a + m_p L_a^2 + m_p l_p^2 \sin^2(\alpha)\right)\ddot{\theta} + m_p L_a l_p \cos(\alpha)\,\ddot{\alpha} + \left(2m_p l_p^2 \sin(\alpha)\cos(\alpha)\,\dot{\alpha} + \frac{k_\tau^2}{R_m}\right)\dot{\theta} - m_p L_a l_p \sin(\alpha)\,\dot{\alpha}^2 = \frac{k_\tau}{R_m} v \tag{1}$$

$$m_p L_a l_p \cos(\alpha)\ddot{\theta} + \left(m_p l_p^2 + J_p\right)\ddot{\alpha} - m_p l_p^2 \sin(\alpha)\cos(\alpha)\dot{\theta}^2 + C_p\dot{\alpha} - m_p g l_p \sin(\alpha) = 0 \tag{2}$$

### 2.2. *Multi-body simulation environment for a lab set-up*

The work developed in this article considers a rotary inverted pendulum available at the Department of Systems Engineering and Automation from the Polytechnic University of Valencia as a study case. The prototype is equipped with a data acquisition board and is easily commanded using Matlab/Simulink.

By using the *Simscape Multibody toolbox*, a 3D simulation environment was constructed for the Furuta pendulum. The multi-body modelling was carried out by performing a mechanical inspection on the laboratory set-up to obtain the physical dimensions of the prototype. Additionally, the electromechanical parameters of the DC motor joined to the arm were deducted from the corresponding data sheet.

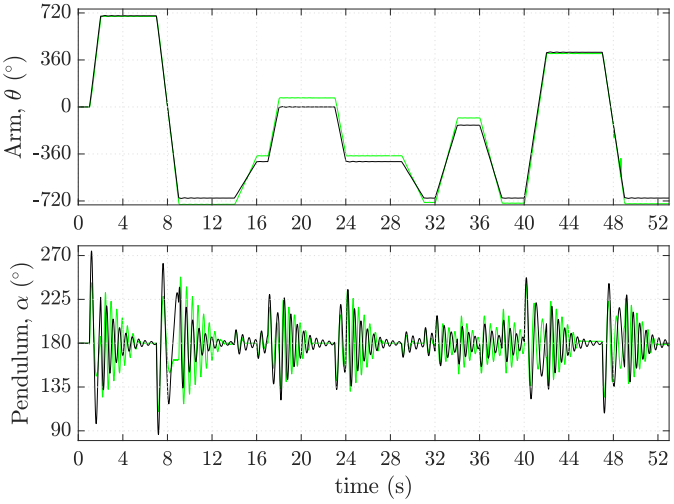


Figura 1: Measured (green) and simulated (black) arm angle ($\theta$) and pendulum angle ($\alpha$) for step changes in the voltage input $0 \leq |v| \leq 5$ V.

In order to validate the simulation environment, a squared signal of voltage with different pulse widths and amplitudes within the range from −5 V to 5 V was applied as input. The arm and pendulum angles were registered from $\theta = 0°$ and $\alpha = 180°$ representing the downward position of the pendulum or the stable equilibrium point.

Figure 1 shows the angles data measured and the outputs obtained from the 3D simulation environment. Notice that the multi-body modelling properly reflects the physical behaviour of the prototype, which indicates that the above can be confidently used to emulate the actual dynamics of the sub-actuated system.

## 3. Constrained closed-loop with active disturbance rejection control and outputs predictions

This section briefly describes the Modified Active Disturbance Rejection Predictive Control (MADRPC) (Martínez, 2023), which allows designing a constrained predictive control law for the Furuta pendulum without its linearised model.

The block diagram of the MADRPC approach is depicted in Figure 2, where it can be seen the information exchange among three main structures: the controlled plant, the disturbance rejector and the modified predictive controller.

### 3.1. *Disturbance rejector*

The disturbance rejector is the disturbance rejection mechanism inherited from the ADRC and it is comprised of the discretised Linear Extended State Observer (LESO) and the sum-gain configuration from which the manipulated variable is computed in Figure 2.

The disturbance rejector enforces first-order plus integrator dynamics defined by a static constant $K$ and an apparent time constant $T$ on the controlled plant. The above is possible because this structure estimates and compensates for the mismatch between the actual system and the assumed dynamics. Consequently, the predictive control law is designed to govern the resultant modified plant.

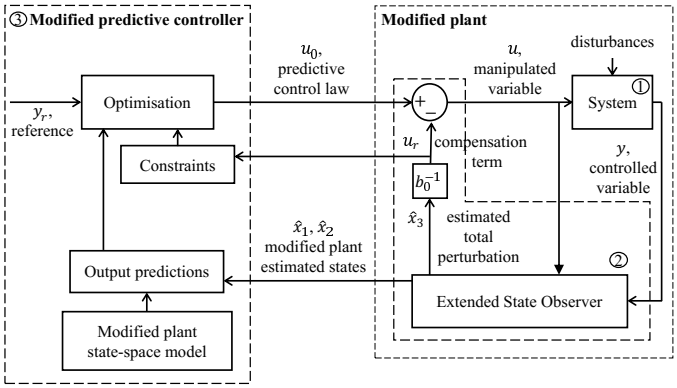


Figura 2: Block diagram of the Modified Active Disturbance Rejection Predictive Control (MADRPC)[Taken from (Martínez, 2023)].

The LESO is implemented in current-observer mode through (3) where $\hat{\mathbf{x}}_k = [\hat{x}_{1,k}, \hat{x}_{2,k}, \hat{x}_{3,k}]^\top$ is the vector of estimated states, $u_k$ is the input, $y_k$ is the measured output, $b_0 \approx K/T$ is the nominal value of the critical gain, and the observer matrices are (4)-(6).

$$\hat{\mathbf{x}}_k = (A_o - \boldsymbol{\ell_o} C_o A_o)\,\hat{\mathbf{x}}_{k-1} + (B_o - \boldsymbol{\ell_o} C_o B_o)\,u_{k-1} + \boldsymbol{\ell_o} y_k \tag{3}$$

$$A_o = \begin{bmatrix} \overbrace{\begin{bmatrix} 1 & T\left(1-e^{-t_s/T}\right) \\ 0 & e^{-t_s/T} \end{bmatrix}}^{A} & \begin{matrix} Tt_s - T^2\left(1-e^{-t_s/T}\right) \\ T\left(1-e^{-t_s/T}\right) \end{matrix} \\ \mathbf{0}_{1\times 2} & 1 \end{bmatrix} \tag{4}$$

$$B_o = b_0 \begin{bmatrix} \overbrace{\begin{bmatrix} Tt_s - T^2\left(1-e^{-t_s/T}\right) \\ T\left(1-e^{-t_s/T}\right) \end{bmatrix}}^{B} \\ 0 \end{bmatrix} \tag{5}$$

$$C_o = \begin{bmatrix} \overbrace{\begin{bmatrix} 1 & 0 \end{bmatrix}}^{C} & 0 \end{bmatrix} \tag{6}$$

The LESO gains vector $\boldsymbol{\ell_o}$ is obtained by solving (7), assuming all poles are at the same location defined by the observer bandwidth $\omega_o$.

$$|zI - (A_o - \boldsymbol{\ell_o} C_o A_o)| = \left(z - e^{-\omega_o t_s}\right)^3 \tag{7}$$

According to (7), with a proper selection of $\omega_o$ the LESO estimates the states $\hat{x}_{1,k}$, $\hat{x}_{2,k}$ of the modified plant and the lumped total perturbation, whose information is contained in $\hat{x}_{3,k}$ and is compensated for through

$$u_k = u_{0,k} - u_{r,k} = u_{0,k} - b_0^{-1}\hat{x}_{3,k} \tag{8}$$

### 3.2. *Modified predictive controller*

This structure computes for each instant $k$ a control action obtained from the minimisation of the cost function (9), which involves the prediction error, the rate of change of the control law, and softening terms. The optimisation problem defined by (9)-(11) uses the compensation term $u_{r,k}$ to redefine the constraints as inequalities so that $F$, and $G$ are matrices of proper dimensions relating the decision variables $\tilde{\mathbf{x}} = [\boldsymbol{\Delta u}\, \xi_1\, \xi_2]^\top$, $\boldsymbol{\Delta u} \in \mathbb{R}^{c\times 1}$, with the vectorial functions $f$, and $g$ dependent on the actual bounds, the reference $y_r$ and the future outputs $y_f$.

$$J_M = \sum_{i=1}^{p} \|y_{r,i|k} - y_{f,i|k}\|_\gamma^2 + \sum_{i=0}^{c-1} \|\Delta u_{0,i|k}\|_\lambda^2 + \sum_{i=1}^{p} \|\xi_{1,i|k}\|_{\varepsilon_1}^2 + \sum_{i=p+1}^{p+2} \|\xi_{2,i|k}\|_{\varepsilon_2}^2 \tag{9}$$

s.t.

$$F\tilde{\mathbf{x}} \leq f\left(\underline{\Delta u}, \overline{\Delta u}, \underline{u}, \overline{u}, \underline{y}, \overline{y}, y_{f,i|k}, u_{r,i|k}\right) \tag{10}$$

$$G\tilde{\mathbf{x}} = g\left(y_{r,i|k}, y_{f,i|k}\right) \tag{11}$$

The modified predictive controller computes the control action $u_{0,k}$ based on the prediction model given by the fixed state-space realisation of the first-order plus integrator plant $(A, B, C, 0)$ from (4)-(6).

## 4. Modified Active Disturbance Rejection Predictive Control for the Furuta pendulum

As stated in section 2, the Furuta pendulum is a sub-actuated system with two controllable outputs, the arm angle and the pendulum angle, and a single manipulated variable, the motor input voltage. Therefore, as shown in Figure 3, the system is controlled by two MADRPC loops in a parallel configuration, where the control action computed for the arm subsystem is subtracted from the control law obtained for the pendulum to produce the driving signal of the prototype. The control goal is to perform reference tracking for the arm angle while stabilising the pendulum in its unstable upward position.

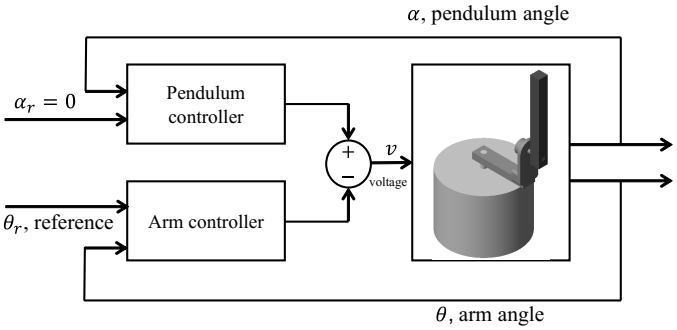


Figura 3: Parallel MADRPC configuration for the Furuta Pendulum.

### 4.1. *Controllers design*

Each of the MADRPC loops to be designed requires the adjustment of two groups of parameters besides the sampling time: on the one hand, those related to the estimation speed and the desired dynamics for the modified plant, and on the other hand, the parameters from the predictive controller that governs on it.

As the MADRPC approach is based on a design free of the identified model, the starting values for the modified plant dynamics are extracted from the system open-loop response. For this purpose, consider Figure 4, which is the measured arm angle when a voltage pulse of 10 V and 0,1 s is applied as input.

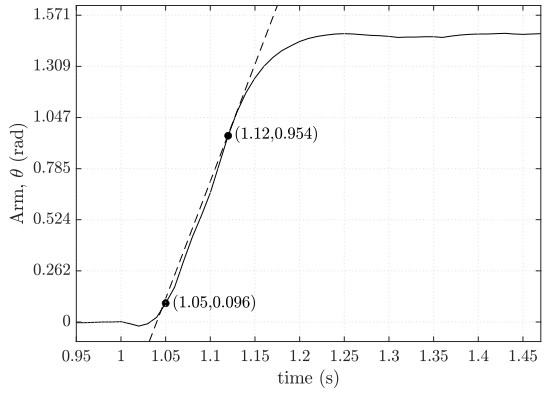


Figura 4: Measured arm angle when a voltage pulse of 10 V is applied as input from $t = 1$ s to $t = 1{,}1$ s.

At first sight, the response reflects integration dynamics in the arm because a steady-state output is obtained with the pulse-type excitation. Two pairs $(t, \theta)$ are marked in Figure 4 to deduce the approximate static gain (12). Besides, the system non-minimum behaviour is perceived in the first instants of the output. Thus, an approximation of an apparent time constant is assumed as the time after which the response becomes monotonic, resulting in $T \approx 0{,}05$ s. Consequently, a first estimation of the nominal value for the critical gain related to the arm MADRPC loop would be $b_0 = K/T \approx 245\,\text{rad}/(\text{V s})$.

$$K = \frac{0{,}954 - 0{,}096}{(1{,}12 - 1{,}05)\,(10)\,(0{,}1)} \approx 12{,}257\,\text{rad/V} \qquad (12)$$

The linearisation of (1)-(2) around the equilibrium points and its transformation in the transfer matrix leads to deduce that the pendulum angle to input transfer function has the same time constants as the arm angle to input transfer function. Therefore, the $T$ value from the arm is assumed for the pendulum MADRPC subsystem.

On the other hand, when the pendulum is held in its unstable position, and the input voltage actions the arm, a negative value for $\alpha$ is measured, which leads to conclude that the nominal value for the pendulum controller should be negative. Its determination is more challenging due to the inherent instability, but the negated $b_0$ value computed for the arm could be also adopted as starting point.

As a remark, the data analysis performed previously is intended to give rough starting values for the required modified plant parameters for both subsystems. However, as discussed in the following subsection, re-tuning the controllers can enhance the closed-loop behaviour.

Finally, the data from Figure 4 was registered at a frequency $f_s = 100$ Hz, so the sampling time $t_s = 10$ ms is maintained for the controllers execution. Moreover, both observer bandwidths were set as $\omega_o = 60\,\text{rad/s}$, approximately ten times lesser than the sampling rate. The complete set of design parameters are reported in Table 2 together with the constraints imposed.

### 4.2. *Simulation results*

The scheme of Figure 3 was implemented in Matlab/Simulink using the 3D multi-body modelling introduced in Section 2 to simulate the actual behaviour of the Furuta pendulum from the laboratory set-up.

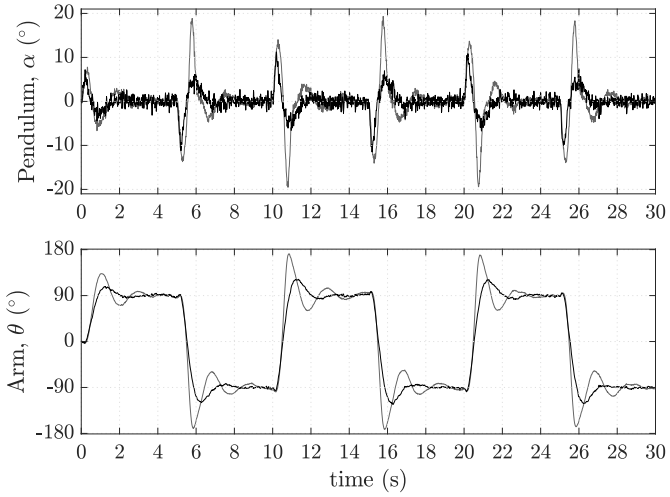


Figura 5: Closed-loop response of the Furuta pendulum controlled by the MADRPC with the initial values ($b_{0i}, T_i$ in gray) and the final tuned parameters ($b_{0f}, T_f$ in black).

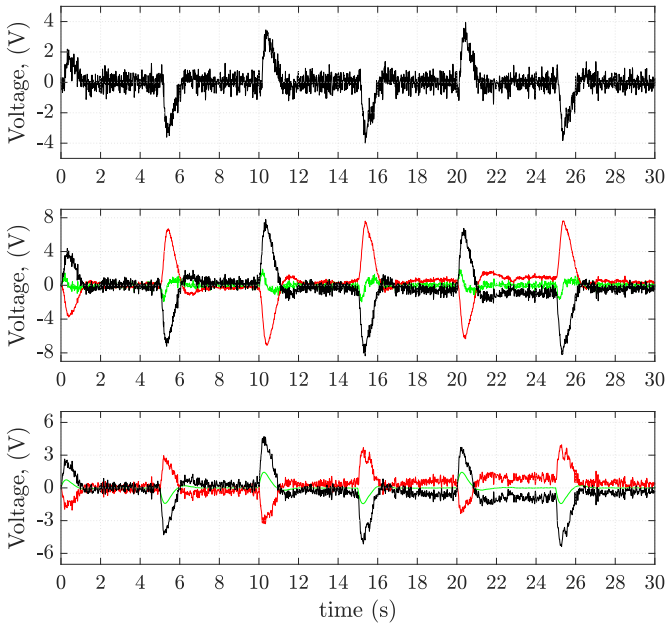


Figura 6: Voltages produced by the MADRPC with the final tuned parameters ($b_{0f}, T_f$) when the reference is set as a squared signal of amplitude 90° and period 10 s.

Additionally, a Gaussian random signal with zero mean and variance $5 \times 10^{-5}$ was added to the system outputs to emulate the measurement noise introduced by the sensors.

Figure 5 presents the closed-loop behaviour of the Furuta pendulum with the designed controllers when the reference for the arm angle is set as a squared signal of period 10 s and amplitude 90°. The results from two scenarios are plotted. In the first one, the system is controlled with the values for the critical gain and time constant deduced in the previous subsection. As shown, with this selection for the modified plant behaviour is possible to hold the pendulum in the vertical upward position overcoming the perturbation caused by the arm rotation.

Tabla 2: MADRPC design for the Furuta pendulum. The sub-indices $i$ and $f$ indicate the initial and final tuned values.

| | Modified predictive controller | | | | | Disturbance rejector | | | | System constraints | | | |
|---|---|---|---|---|---|---|---|---|---|---|---|---|---|
| Controller | $c$ | $p$ | $\lambda$ | $\gamma$ | $\varepsilon_1, \varepsilon_2$ | $b_{0i}$ | $b_{0f}$ | $T_i$ | $T_f$ | $\omega_o$ | rate of input | input | output |
| Pendulum | 10 | 50 | 58 | 0,5 | $1 \times 10^5$ | $-245$ | $-100$ | 0,05 | 0,1 | 60 | $\lvert\Delta v\rvert \leq 1$ | $\lvert v\rvert \leq 10$ | $\lvert\alpha\rvert \leq 30°$ |
| Arm | 60 | 100 | 0,06 | 100 | $1 \times 10^5$ | 245 | 50 | 0,05 | 0,1 | 60 | $\lvert\Delta v\rvert \leq 1$ | $\lvert v\rvert \leq 10$ | $\lvert\theta\rvert \leq 180°$ |

In a second scenario, a re-tuning of $b_0$ and $T$ results in a stable closed-loop response that causes less deviation from the vertical for the pendulum and a faster movement for the arm which reaches the desired angle in about 2 s despite the slight overshoot produced.

The corresponding voltages produced with the final tuning are plotted in Figure 6. The first row is the input applied to the motor driving the arm. The second and third rows present the control signals computed for the pendulum MADRPC loop and the arm MADRPC loop, respectively. In each case, the manipulated variable of the subsystem $u = u_0 - u_r$ (black) is obtained by combining the predictive law $u_0$ (green) with the compensation term $u_r$ (red).

On the one hand, from Figure 6 it is deduced that the Disturbance rejector properly estimates and compensates for the discrepancies between the Furuta pendulum dynamics and the first-order plus integrator state-space realisations assumed as modified plants in each loop. Moreover, the Modified predictive controllers compute control laws satisfying the imposed constraints. On the other hand, the overshoot produced in the arm angle from Figure 5 reflects the process non-linearity and a more dedicated tuning procedure should be required to improve the performance.

## 5. Conclusions

This work addressed the design of predictive control laws subject to constraints for the control of a sub-actuated, non-minimum phase, and highly non-linear benchmark system without the need to include the modelling dynamics in the optimisation process. Instead, the design is developed based on the MADRPC, which actively estimates and compensates for the mismatch between the actual controlled process and an assumed prediction model resembling first-order plus integrator dynamics. This formulation allows the incorporation of constraints for the system variables while assuring feasibility and stability.

The results were obtained by implementing the designed loop to control a 3D Simscape multi-body environment that accurately reflects the actual dynamics of a Furuta pendulum from a laboratory set-up. Therefore, the MADRPC strategy is validated in a mechanical plant expanding its applicability to SIMO processes.

No modelling was performed for the loop design. The deduction of the tuning parameters related to the prediction model is discussed based on a test carried out on the open-loop system.

Proper control of both outputs of the Furuta pendulum was obtained with the designed control. However, analysing tuning alternatives for the methodology considering the desired performance is identified as future work.

## Acknowledgement

This work has been partly supported by Ministry of Science, Technology and Innovation of Colombia [Scholarship 885], GVA Regional Government [Project CIAICO/2021/064], MCIN/AEI/10.13039/501100011033 [Project PID2020-120087GB-C21], and MCIN/AEI/10.13039/501100011033 [Project PID2020-119468RA-I00].

## Referencias

Cazzolato, B. S., Prime, Z., 2011. On the dynamics of the furuta pendulum. Journal of Control Science and Engineering 2011, 1–8.

Chen, Q., Zhuang, J., Liu, B., Yang, P., 2022. Inverted pendulum balance control based on improved active disturbance rejection control. In: 2022 China Automation Congress (CAC). IEEE, pp. 1526–1531.

Diwan, S. P., Deshpande, S. S., 2022. A hybrid optimizer based nonlinear model predictive control for rotary inverted pendulum. In: 2022 International Conference on Automation, Computing and Renewable Systems (ICACRS). IEEE, pp. 121–127.

Hamza, M. F., Yap, H. J., Choudhury, I. A., Isa, A. I., Zimit, A. Y., Kumbasar, T., 2019. Current development on using rotary inverted pendulum as a benchmark for testing linear and nonlinear control algorithms. Mechanical Systems and Signal Processing 116, 347–369.

Han, J., 2009. From PID to active disturbance rejection control. IEEE Transactions on Industrial Electronics 56, 900–906.

Homburger, H., Wirtensohn, S., Reuter, J., 2022. Swinging up and stabilization control of the furuta pendulum using model predictive path integral control. In: 2022 30th Mediterranean Conference on Control and Automation (MED). IEEE, pp. 7–12.

Liu, B., Hong, J., Wang, L., 2019. Linear inverted pendulum control based on improved ADRC. Systems Science & Control Engineering 7, 1–12.

Madrid, J. L. D., Querubín, E. A. G., Henao, P. A. O., 2019. MPC in space state for the control of a furuta pendulum. In: Lecture Notes in Mechanical Engineering. Springer Singapore, pp. 219–235.

Martínez, B. V., 2023. Design of controllers based on active disturbance rejection control (adrc) and its integration with model predictive control (mpc). Ph.D. thesis, Universitat Politècnica de València, Valencia, Spain.

Onen, U., 2023. Model-free controller design for nonlinear underactuated systems with uncertainties and disturbances by using extended state observer based chattering-free sliding mode control. IEEE Access 11, 2875–2885.

Prado, A., Herrera, M., Menéndez, O., 2020. Intelligent swing-up and robust stabilization via tube-based nonlinear model predictive control for a rotational inverted-pendulum system. Revista Politécnica 45, 49–64.

Ramirez-Juarez, R., Ramírez-Neria, M., Luviano-Juárez, A., 2021. Tracking trajectory control of a double pendulum gantry crane using ADRC approach. In: Advances in Automation and Robotics Research. Springer International Publishing, pp. 92–100.

Ramírez-Neria, M., Sira-Ramírez, H., Garrido-Moctezuma, R., Luviano-Juárez, A., 2014. Linear active disturbance rejection control of underactuated systems: The case of the furuta pendulum. ISA Transactions 53, 920–928.

Seman, P., Rohal'-Ilkiv, B., Juhás, M., Salaj, M., 2013. Swinging up the furuta pendulum and its stabilization via model predictive control. Journal of Electrical Engineering 64, 152–158.

Xian, J., Haichen, Z., Ming, W., 2020. Implementation of linear/nonlinear auto disturbance rejection switching control in inverted pendulum system. In: Proceedings of the 2020 2nd International Conference on Robotics, Intelligent Control and Artificial Intelligence. ACM, pp. 393–397.